doi: 10.15407/ujpe60.12.1224

YU.A. ROMANYUK, A.M. YAREMKO, V.M. DZHAGAN, V.O. YUKHYMCHUK

V.E. Lashkaryov Institute of Semiconductor Physics, Nat. Acad. of Sci. of Ukraine
(45, Prosp. Nauky, Kyiv 03028, Ukraine; e-mail: romanyuk_yu@ukr.net)

PACS 42.65.Dr, 68.65.Hb, 73.21.La

RAMAN SCATTERING IN SUPERLATTICES WITH Ge QUANTUM DOTS

The studies of the Raman scattering in superlattices with layers of Ge quantum dots (QDs) are carried out. A theoretical model describing the experimental spectra with regard for the real crystal structures of both the QD and the surrounding matrix, as well as the phonon-phonon interaction in the matrix and in the QDs, is proposed. The intensities of Raman spectra are calculated with the use of the secondary quantization procedure and Green's functions. The results obtained show that the crystal structure of the superlattice composed of alternating silicon layers and layers with Ge quantum dots can be described as a mixed crystal consisting of a matrix with a certain distribution of "impurities" ("Ge-molecules"). A qualitative correlation between the theoretically calculated and experimentally measured positions and intensities of bands in the Raman spectra of QD superlattices is demonstrated, and the doublet character of the bands is explained.

K e y w o r d s: quantum dot, superlattice, Raman scattering, Green's function, phonons.

1. Introduction and Statement of the Problem

For two last decades, the electronic and optical properties of quantum-dimensional crystal structures have been intensively studied, what created preconditions for their practical application as promising materials in modern nano- and optoelectronics [1–3]. If the dimensions of quantum dots (QDs) approach the Bohr radius of excitons in them, the fundamental properties of QDs start to substantially differ from the corresponding parameters of bulk crystals. In view of the importance of understanding the physical processes running in QDs and superlattices (SLs), they have been studied for a long time both experimentally and theoretically [1–16].

In earlier theoretical works [4, 7], a linear chain was taken as a basis for the description of the Raman spectra experimentally measured from SLs consisting of quantum-dimensional layers. The appearance of a number of additional bands in the interval of acoustic oscillations in the Raman spectra was explained as the effect of growing a crystal unit cell. This model was successfully used to calculate the dispersion relations for acoustic and optical phonons in GaAs/AlAs and InAs/GaAs superlattices [6]. Numerical calculations of the dispersion of phonon branches (both acoustic and optical) for SLs were carried out in work [5].

The propagation of acoustic vibrations in a periodic layered medium was considered for the first time by S.M. Rytov [10]. In his model, the dispersion of acoustic phonons coincides with the dispersion obtained in the framework of the linear chain model for phonons in a low-frequency spectral range. The difference for high-frequency phonons is connected with the nonlinearity of their dispersion in this interval. More complicated theoretical researches of the dispersion relations for vibrations in SLs and their dependences on the SL parameters were performed in

works [12, 13]. However, vibrations in such structures were described in the framework of the macroscopic model, when the density and the elastic constants of the medium change periodically in space.

The appearance of SLs with QD layers stimulated the intensive researches of their properties [17–20]. One of the first studies in this direction was work [17] dealing with CdSe nanospheres. The consideration was carried out in the framework of a classical model, in which nanospheres with radius r and dielectric permittivity ε were embedded into a matrix with dielectric permittivity ε_d. In works [18, 19], QDs were considered as homogeneous spheres. Vibrations in them were described by the Navier equations with special boundary conditions. As a result, vibrations of two types in QDs were obtained: spherical and torsional ones.

Another approach to the problem was proposed in work [20]. The QD was considered to be a homogeneous cylindrical disk with a circular or elliptic cross-section oriented perpendicularly to the axis. According to the proposed model, QDs interact with one another by means of acoustic vibrations [21, 25–29]. The calculations of the Raman scattering spectra were made with the help of the deformation potential of interaction between acoustic phonons and electron states localized in the QDs. On the basis of the results obtained, a conclusion was drawn that the bands observed in the Raman spectra are associated with the interference of light scattered by different QD layers in the SL.

One more theoretical consideration of the spectrum of optical phonons in QDs was carried out in the framework of the valence force field model [22, 23]. This model is empirical and allows the phonon frequencies in QDs consisting of several thousands of atoms to be calculated. For the calculations in the framework of this model, large data arrays are required, which makes the calculations rather laborious.

In work [24], the model of dielectric continuum was applied to describe the Raman scattering spectra, while studying SLs. However, this model is a macroscopic approximation.

Therefore, despite a considerable number of works devoted to the simulation of Raman scattering spectra obtained from superlattices with QD layers, the problem of their description remains challenging. In our research, the experimental Raman spectra will be described at the microscopic level, i.e. the real atomic

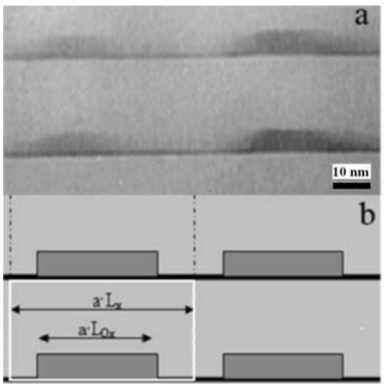

Fig. 1. TEM image of Ge quantum dots in a silicon matrix (a), schematic diagram of a new cell in the SL with QDs: L_x is the number of old unit cells in the new unit cell, and L_{0x} the number of old unit cells in the QD (b)

structures of QDs and the matrix will be made allowance for. Since the lattice constants a for Ge and Si are close (in particular, $\Delta a/a \approx 0.04$ for the corresponding values) and the QD size d is rather big ($d \gg a$), a new cell can be introduced, which includes a Ge quantum dot and, partially, the surrounding Si matrix, as is illustrated in Fig. 1. The new unit cell is large enough to include many of old cells, each containing a QD in the Si matrix. Assuming that the lattice constants are identical in the zeroth-order approximation, we obtain a new crystal with a different lattice parameter, $a \to La$, where $L = \{L_x, L_y, L_z\}$. It is important that the approximate equality between the Ge and Si lattice constants means the same reciprocal lattice vector $k = 2\pi/a$ for the whole crystalline structure.

Dispersion curves of acoustic phonons for the majority of SL materials overlap in rather a wide frequency interval. Therefore, acoustic phonons from different layers propagate freely through the whole crystal structure. The new crystal periodicity results in the convolution of dispersion phonon branches in the new Brillouin zone. If the dispersion branches of optical phonons lie in different spectral ranges, the optical phonons turn out localized in a certain layer. In this case, the optical phonons inherent to one material cannot propagate in layers of another material and quickly fade out at a distance of one or two monolayers from the interface. Such phonons do not reveal a dispersion in the direction normal to the nanostructure layers and can be regarded as standing waves localized in each layer.

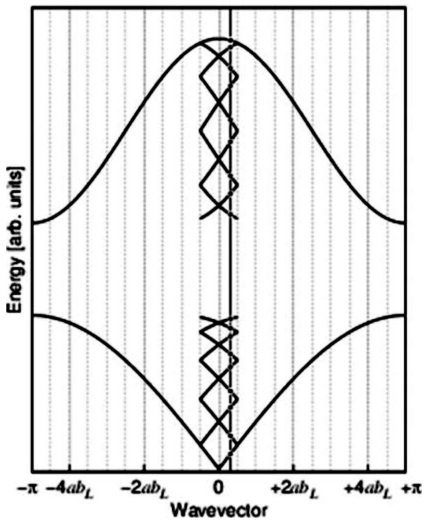

Fig. 2. Change of phonon dispersion branches at the increase in the lattice constant $a \to aL$ (the case $L = 10$ is shown)

A model proposed in this work allows the features in the Raman spectra of phonons of all types to be analyzed in the framework of the microscopic approach, using only the general parameters of real crystals, including phonon frequencies, atomic masses, and lattices constants. It is evident that, in the SL with QDs, the number of optical phonons grows, because the new reciprocal lattice vector b_L is shorter than that determined in the wide Brillouin zone, $b = 2\pi/a \to b_L = 2\pi/(La)$. Therefore, every optical dispersion branch in the wide Brillouin zone transforms into several optical branches in the new zone, and every acoustic branch transforms into one acoustic branch and several optical ones (Fig. 2). As a result, there appear a lot of new optical low-frequency phonons in the Raman spectrum, which are caused by the formation of large crystal cells. It should be noted that the dispersion of optical phonons, as a rule, is low; therefore, some new components may not manifest themselves in the spectrum, but the phonon band should become asymmetric (according to Fig. 2, toward the low-frequency side).

2. Theory

2.1. Hamiltonian of the crystal

The Hamiltonian of the crystal consists of several components that characterize the electron subsystem energy, $H_{\rm el}$, the energy of vibrations, $H_{\rm ph}$, and the energy of electron-phonon interaction, $H_{\rm el-ph}$. In this work, the processes of non-resonant Raman scattering are analyzed. Therefore, the consideration can be confined to the phonon part of the Hamiltonian only. In the second-quantization representation and the harmonic approximation, the Hamiltonian can be written as follows:

$$
\begin{aligned}
H = &\sum_{\tilde{q},g,s_1} \omega_{\tilde{q}+g,s_1} b^{+}_{\tilde{q}+g,s_1} b_{\tilde{q}+g,s_1} + \\
&+ \sum_{\tilde{q},g,s_0} \omega_{\tilde{q}+g,s_0} b^{+}_{\tilde{q}+g,s_0} b_{\tilde{q}+g,s_0} - \\
&- \frac{1}{2} \sum_{\tilde{q},g,s_0,g',s'_0} \Bigg[T^{(0)}_{\tilde{q}}\binom{s_0,s'_0}{g,g'} \delta_{g,g'} - \\
&- \Delta T^{(0)}_{\tilde{q}}\binom{s_0,s'_0}{g,g'} a^{L_0}_{(g'-g)} \Bigg] \pi_{-(g+\tilde{q}),s_0} \pi^{+}_{-(g'+\tilde{q}),s'_0} \Bigg] - \\
&- \frac{1}{2} \sum_{\tilde{q},g,s_1,g',s'_1} \Delta T^{(1)}_{\tilde{q}}\binom{s_1,s'_1}{g,g'} a^{L_0}_{(g'-g)} \pi_{-(g+\tilde{q}),s_1} \pi^{+}_{-(g'+\tilde{q}),s'_1} - \\
&- \frac{1}{2} \sum_{\tilde{q},g,s_0,g',s'_0} \Bigg[\delta_{g,g'} L \bar{V}_{\tilde{q}}\binom{s_0,s'_0}{g,g'} - a^{L_0}_{g+\tilde{q}} a^{*L_0}_{g'+\tilde{q}} L V_{\tilde{q}}\binom{s_0,s'_0}{g,g'} \Bigg] \times \\
&\times \varphi_{g+\tilde{q},s_0} \varphi^{+}_{g'+\tilde{q},s'_0} \Bigg] - \frac{1}{2} \sum_{\tilde{q},g,s_1,g',s'_1} \Bigg[(a^{L}_{g+\tilde{q}} - a^{L_0}_{g+\tilde{q}}) a^{*L_0}_{g'+\tilde{q}} + \\
&+ a^{L_0}_{g+\tilde{q}} (a^{*L}_{g'+\tilde{q}} - a^{*L_0}_{g'+\tilde{q}}) + a^{L_0}_{g+\tilde{q}} a^{*L_0}_{g'+\tilde{q}} \Bigg] \times \\
&\times L V_{\tilde{q}}\binom{s_1,s'_1}{g,g'} \varphi_{g+\tilde{q},s_1} \varphi^{+}_{g'+\tilde{q},s'_1} + \frac{1}{2} \sum_{\tilde{q},g,s_1,g',s'_1} (a^{L}_{g+\tilde{q}} - a^{L_0}_{g+\tilde{q}}) \times \\
&\times a^{*L_0}_{g'+\tilde{q}} L V_{\tilde{q}}\binom{s_1,s'_0}{g,g'} \varphi_{g+\tilde{q},s_1} \varphi^{+}_{g'+\tilde{q},s'_0} + \\
&+ \frac{1}{2} \sum_{\tilde{q},g,s_1,g',s'_1} a^{L_0}_{g+\tilde{q}} (a^{*L}_{g'+\tilde{q}} - a^{*L_0}_{g'+\tilde{q}}) \times \\
&\times L V_{\tilde{q}}\binom{s_0,s'_1}{g,g'} \varphi_{g+\tilde{q},s_0} \varphi^{+}_{g'+\tilde{q},s'_1}. \qquad (1)
\end{aligned}
$$

The Hamiltonian is written in such a form that the real crystal structure is presented as two virtual Ge and Si crystals, each with the volume $V = v_0 N$, where v_0 and N are the volume and the number of unit cells, respectively [30]. The meaning of every term in expression (1) is as follows: the first two terms describe the Hamiltonians of both crystals, Si and Ge, characterized by the subscripts 1 and 0, respectively; the third and fourth terms describe the excitation related to the kinetic energy of crystals, $T^{(0)}$, $\Delta T^{(0)}$, and $\Delta T^{(1)}$; and the last four terms are connected with the potential energy of the real crystal structure, which is presented as a sum

$$V = V^{00} + V^{11} + (\Delta V^{00} + \Delta V^{11} + \Delta V^{10} + \Delta V^{01}).$$

In the operators of normal coordinates,

$$\varphi_{q,s} = \frac{1}{\sqrt{2}}(b_{q,s} + b^{+}_{-q,s}) = \varphi^{+}_{-q,s},$$

and corresponding momenta,

$$\pi_{q,s} = \frac{1}{\sqrt{2}}(b^{+}_{q,s} - b_{-q,s}) = -\pi^{+}_{-q,s},$$

of lattice vibrations, the wave vector q looks like $q = g + \tilde{q}$, where g is the wave vector of the new reciprocal lattice, and the wave vector $\tilde{q}$ changes within different limits $(-\pi/aL_j \leqslant \tilde{q}_j \leqslant \pi/aL_j,\ j = x, y, z)$ in this structure. The corresponding phonon branches are enumerated by the index $s_j = s_0$ for the QD and $s_j = s_1$ for the matrix; the oscillating quantities $a^{L_0}_{g+\tilde{q}} = \frac{L_0}{L} f^{L_0}_{g+\tilde{q}}$, where $f^{L_0}_{g+\tilde{q}} = \frac{1}{L_0} \sum\limits_{n_0=1}^{L_0} \exp[i(\tilde{q} + + b_g)n_0]$, depend on the QD dimensions, i.e. on the number n_0 of "old" crystal cells in the QD.

2.2. Raman spectrum intensity and the equation for Green's functions

The intensity of Raman spectra can be expressed by the imaginary part of the Fourier component of the retarded Green's function (GF) for the scattering tensor $\bar{\chi}_{k,\lambda,k',\lambda'}$ [30–32],

$$I_{p',\lambda',p,\lambda} \sim -[1+n(\omega)]\mathrm{Im}\langle\langle \bar{\chi}_{p',\lambda',p,\lambda}(t), \bar{\chi}^{+}_{p',\lambda',p,\lambda}(0)\rangle\rangle_{\omega}, \tag{2}$$

where

$$\begin{aligned} \bar{\chi}_{k,\lambda.k',\lambda'} &= \sum_{\alpha,\beta} \bar{e}_{\alpha}(k,\lambda)\bar{e}^{*}_{\beta}(k',\lambda')\chi_{\alpha,\beta}(Q = k' - k), \\ \chi_{\alpha,\beta}(Q) &= \sum_{p,\gamma} \chi_{\alpha,\beta}(n)\exp(-iQn), \end{aligned} \tag{3}$$

and $\bar{e}_{\alpha}(k,\lambda)$ and $\bar{e}_{\beta}(k',\lambda')$ are the unit vectors of the electric field vectors of the incident and scattered light, respectively. It can be shown that, for the analyzed crystal structure with QDs, the tensor $\chi_{\alpha,\beta}(Q)$ looks like

$$\chi_{\alpha,\beta}(Q) = \sqrt{LN_0}\Bigg\{\sum_{g,s_0} \tilde{\chi}^{s_0}_{\alpha,\beta}(b_g + Q)a^{L_0}_{g}\varphi_{g+Q,s_0} + + \sum_{g,s_1} \tilde{\chi}^{s_1}_{\alpha,\beta}(b_g + Q)[\delta_{g,0} - a^{L_0}_{g}]\varphi_{g+Q,s_1}\Bigg\}, \tag{4}$$

where $N = LN_0$, and N_0 is the number of new large cells.

From Eqs. (2)–(4), it is possible to find the spectral dependence for the light scattering intensity, which is expressed in terms of the Fourier component of the GF for phonon operators. Below, in order to simplify the understanding, we consider a case where only one phonon branch ($s_0 = \alpha_0$ and $s_1 = \alpha_1$) is actual for the Ge and Si crystals. Then, the intensity of light scattering can be expressed as follows:

$$\begin{aligned} &I_{p',\lambda',p,\lambda}(\omega) \sim \\ &\sim -[1+n(\omega)]\frac{1}{\tilde{N}}\mathrm{Im}\Bigg\{\sum_{g} \tilde{\chi}^{\alpha_0}_{p',\lambda',p,\lambda}(b_g + Q)a^{L_0}_{g} \times \\ &\times \sum_{g'} \tilde{\chi}^{*\alpha_0}_{p',\lambda',p,\lambda}(b_{g'} + Q)a^{*L_0}_{g'} \times \\ &\times \langle\langle \varphi_{g+Q,\alpha_0}(t); \varphi^{+}_{g'+Q,\alpha_0}(0)\rangle\rangle_{\omega} + \\ &+ \sum_{g} \tilde{\chi}^{\alpha_0}_{p',\lambda',p,\lambda}(b_g + Q)a^{L_0}_{g} \times \\ &\times \sum_{g'} \tilde{\chi}^{*\alpha_0}_{p',\lambda',p,\lambda}(b_{g'} + Q)[\delta_{g',0} - a^{*L_0}_{g'}] \times \\ &\times \langle\langle \varphi_{g+Q,\alpha_0}(t); \varphi^{+}_{g'+Q,\alpha_1}(0)\rangle\rangle_{\omega} + \\ &+ \sum_{g} \tilde{\chi}^{\alpha_1}_{p',\lambda',p,\lambda}(b_g + Q)[\delta_{g,0} - a^{L_0}_{g}] \times \\ &\times \sum_{g'} \tilde{\chi}^{*\alpha_0}_{p',\lambda',p,\lambda}(b_{g'} + Q)a^{*L_0}_{g'} \times \\ &\times \langle\langle \varphi_{g+Q,\alpha_1}(t); \varphi^{+}_{g'+Q,\alpha_0}(0)\rangle\rangle_{\omega} + \\ &+ \sum_{g} \tilde{\chi}^{\alpha_1}_{p',\lambda',p,\lambda}(b_g + Q)[\delta_{g,0} - a^{L_0}_{g}] \times \\ &\times \sum_{g'} \tilde{\chi}^{*\alpha_1}_{p',\lambda',p,\lambda}(b_{g'} + Q)[\delta_{g',0} - a^{*L_0}_{g'}] \times \\ &\times \langle\langle \varphi_{g+Q,\alpha_1}(t); \varphi^{+}_{g'+Q,\alpha_1}(0)\rangle\rangle_{\omega}\Bigg\}. \end{aligned} \tag{5}$$

Relation (5) shows that the intensity of light scattering is expressed in terms of the Fourier components of the retarded GF for phonon operators of the type $\varphi_{g+Q,s}$, where Q is the wave vector of incident radiation. Below, we will use the phonon operators $\varphi_{p+k,\alpha}$, where α characterizes the phonon branches of either the QD ($\alpha = \alpha_0$) or the matrix ($\alpha = \alpha_1$).

The GF is described by the following expression:

$$\begin{aligned} &\langle\langle \varphi_{p+k,\alpha}(t); \varphi^{+}_{p'+k',\alpha}(0)\rangle\rangle = \\ &= -i\Theta(t)\langle[\varphi_{p+k,\alpha}(t); \varphi^{+}_{p'+k',\alpha'}(0)]\rangle, \end{aligned} \tag{6}$$

where $\Theta(t)$ is the step function, [...; ...] means the commutator of two operators, $\langle ... \rangle$ is the statistical averaging of operators, and $\varphi_{p+k,\alpha}(t) = \exp(iHt)\varphi_{p+k,\alpha}\exp(-iHt)$. The equation for the GF looks like

$$i\frac{\partial}{\partial t}\langle\langle\varphi_{p+k,\alpha}(t);\varphi^{+}_{p'+k',\alpha'}(0)\rangle\rangle =$$
$$= \delta(t)\langle[\varphi_{p+k,\alpha}(0);\varphi^{+}_{p'+k',\alpha'}(0)]\rangle +$$
$$+ \langle\langle i\frac{\partial}{\partial t}\varphi_{p+k,\alpha}(t);\varphi^{+}_{p'+k',\alpha'}(0)\rangle\rangle, \quad (7)$$

where $\varphi_{-(p+k),\alpha} = \varphi^{+}_{p+k,\alpha}$, and the commutator $[\varphi_{p+k,\alpha}(0);\varphi^{+}_{p'+k',\alpha'}(0)] = 0$. Since the first term in expression (7) equals zero, only the last one gives a contribution to the GF.

The operator derivative depends on Hamiltonian (1) and is described by the expression

$$i\frac{\partial}{\partial t}\varphi_{p+k,\alpha}(t) = [\varphi_{p+k,\alpha}; H_0 + \Delta H], \quad \alpha = \{\alpha_1,\ \alpha_0\}, \quad (8)$$

in which

$$H_0 = \sum_{\tilde{q},g,\beta}\omega_{\tilde{q}+g,\beta}b^{+}_{\tilde{q}+g,\beta}b_{\tilde{q}+g,\beta},\quad \beta = \{s_1, s_0\}. \quad (9)$$

Other terms in expression (1) are a perturbation resulting from the non-ideality of the initial crystal, and they give rise to a system of coupled equations for the GF.

Below, we will assume that, as was indicated above, each of the matrix and the QDs (i.e. the crystals consisting of the QD and matrix materials) has only one (optical or acoustic) vibration mode, and the constants characterizing the interaction between the phonons with the wave vector $g + k$ from the branch α and the phonons with the wave vector $p + k$ from the branch β do not depend on the wave vectors, $LV_k\binom{\alpha,\beta}{g,p} = V^{\alpha,\beta}$.

To analyze the equations for GF, the following notations are introduced:

$$G^{L_0}_{\alpha_0,k,\alpha',p'+k'} = \sum_{g_1} a^{L_0}_{g_1+k}\langle\langle\varphi_{g_1+k,\alpha_0}(t);\varphi^{+}_{p'+k',\alpha'}(0)\rangle\rangle_\omega, \quad (10a)$$

$$G^{L-L_0}_{\alpha_1,k,\alpha',p'+k'} = \sum_{g_1}(a^{L}_{g_1+k} - a^{L_0}_{g_1+k})\langle\langle\varphi_{g_1+k,\alpha_1}(t);\varphi^{+}_{p'+k',\alpha'}(0)\rangle\rangle_\omega, \quad (10b)$$

$$G^{L_0}_{\alpha_1,k,\alpha',p'+k'} = \sum_{g_1} a^{L_0}_{g_1+k}\langle\langle\varphi_{g_1+k,\alpha_1}(t);\varphi^{+}_{p'+k',\alpha'}(0)\rangle\rangle_\omega. \quad (10c)$$

Then, two equations for the Fourier components of GF read

$$\langle\langle\varphi_{p+k,\alpha_0}(t);\varphi^{+}_{p'+k',\alpha'}(0)\rangle\rangle_\omega = \frac{1}{\Delta(\omega,p+k,\alpha_0)}\times \left\{\tilde{\omega}_{p+k,\alpha_0}\delta_{\alpha_0,\alpha'}\delta_{p+k,p'+k'} + \tilde{\omega}_{p+k,\alpha_0}a^{*L_0}_{p+k}\times [V^{\alpha_0\alpha_0}G^{L_0}_{\alpha_0,k,\alpha',p'+k'} + V^{\alpha_1\alpha_0}G^{L-L_0}_{\alpha_1,k,\alpha',p'+k'}]\right\}, \quad (11a)$$

$$\langle\langle\varphi_{p+k,\alpha_1}(t);\varphi^{+}_{p'+k',\alpha'}(0)\rangle\rangle_\omega = \frac{1}{\Delta(\omega,p+k,\alpha_1)}\{\tilde{\omega}_{p+k,\alpha_1}\delta_{\alpha_1,\alpha'}\delta_{p+k,p'+k'} - \tilde{\omega}_{p+k,\alpha_1}[V^{\alpha_1\alpha_1}a^{*L}_{p+k}G^{L_0}_{\alpha_1,k,\alpha',p'+k'}) - (a^{*L}_{p+k} - a^{*L_0}_{p+k})V^{\alpha_0\alpha_1}G^{L_0}_{\alpha_0,k,\alpha',p'+k'}]\}, \quad (11b)$$

where

$$\tilde{\omega}_{p+k,\alpha_0} = \omega_{p+k,\alpha_0}a^{L_0}_0, \Delta(\omega,p+k,\alpha_0) = \omega^2 - \eta_0\omega_{p+k,\alpha_0}\tilde{\omega}_{p+k,\alpha_0}, (\eta_0 \to 0), \quad (12a)$$

$$\tilde{\omega}_{p+k,\alpha_1} = \omega_{p+k,\alpha_1}(1 - a^{L_0}_0), \Delta(\omega,p+k,\alpha_1) = \omega^2 - \eta_1\omega_{p+k,\alpha_1}\tilde{\omega}_{p+k,\alpha_1}, (\eta_1 = 1). \quad (12b)$$

Relations (12) make it possible to obtain a system of equations for all functions (10). Multiplying Eq. (10a) by $a^{L_0}_{p+k}$ and summing up the result over the subscript p, we obtain

$$G^{L_0}_{\alpha_0,k,\alpha',p'+k'}[1 - f^{L_0L_0}_{\alpha_0}(\omega,k)V^{\alpha_0\alpha_0}] - G^{L-L_0}_{\alpha_1,k,\alpha',p'+k'}f^{L_0L_0}_{\alpha_0}(\omega,k)V^{\alpha_1\alpha_0} = A^{L_0}_{\alpha_0,k,\alpha',p'+k'}, \quad (13)$$

where

$$f^{L_0,L_0}_{\alpha_0}(\omega,k) = \sum_p \frac{a^{L_0}_{p+k}a^{*L_0}_{p+k}\tilde{\omega}_{p+k,\alpha_0}}{\Delta(\omega,p+k,\alpha_0)}, \quad (14a)$$

$$A^{L_0}_{\alpha_0,k,\alpha',p'+k'} = \sum_p a^{L_0}_{p+k}\frac{\delta_{p,p'}\delta_{k,k'}}{\Delta(\omega,p+k,\alpha_0)}\tilde{\omega}_{p+k,\alpha_0}\delta_{\alpha_0,\alpha'} =$$

$$= \frac{a^{L_0}_{p'+k'}\tilde{\omega}_{p'+k',\alpha_0}}{\Delta(\omega, p'+k', \alpha_0)}\delta_{\alpha_0,\alpha'}\delta_{k,k'}. \quad (14b)$$

From Eq. (11b), two other equations can be obtained in the same way, which relate functions (10) with each other. Multiplying Eq. (11b) by the factors $a^{L_0}_{p+k}$ and $(a^{L}_{p+k} - a^{L_0}_{p+k})$, and summing up the result over p, we obtain

$$- G^{L_0}_{\alpha_0,k,\alpha',p'+k'} f^{L_0,L-L_0}_{\alpha_1}(\omega,k)V^{\alpha_0\alpha_1} +$$
$$+ G^{L-L_0}_{\alpha_1,k,\alpha',p'+k'} f^{L_0,L_0}_{\alpha_1}(\omega,k)V^{\alpha_1\alpha_1} + G^{L_0}_{\alpha_1,k,\alpha',p'+k'} \times$$
$$\times [1 + f^{L_0,L}_{\alpha_0}(\omega,k)V^{\alpha_1\alpha_1}] = A^{L_0}_{\alpha_1,k,\alpha',p'+k'}, \quad (15)$$

$$- G^{L_0}_{\alpha_0,k,\alpha',p'+k'} f^{L-L_0,L-L_0}_{\alpha_1}(\omega,k)V^{\alpha_0\alpha_1} +$$
$$+ G^{L-L_0}_{\alpha_1,k,\alpha',p'+k'}[1 + f^{L-L_0,L_0}_{\alpha_1}(\omega,k)V^{\alpha_1\alpha_1}] +$$
$$+ G^{L_0}_{\alpha_1,k,\alpha',p'+k'} f^{L-L_0,L}_{\alpha_0}(\omega,k)V^{\alpha_1\alpha_1} =$$
$$= A^{L-L_0}_{\alpha_1,k,\alpha',p'+k'}, \quad (16)$$

$$f^{L-L_0,L_0}_{\alpha_0}(\omega,k) = \sum_p \frac{(a^{L}_{p+k} - a^{L_0}_{p+k})a^{*L_0}_{p+k}\tilde{\omega}_{p+k,\alpha_0}}{\Delta(\omega, p+k, \alpha_0)}, \quad (17a)$$

$$f^{L-L_0,L-L_0}_{\alpha_0}(\omega,k) =$$
$$= \sum_p \frac{(a^{L}_{p+k} - a^{L_0}_{p+k})(a^{*L}_{p+k} - a^{*L_0}_{p+k})\tilde{\omega}_{p+k,\alpha_0}}{\Delta(\omega, p+k, \alpha_0)}. \quad (17b)$$

Note that the exact solution of the system of equations (13), (15), and (16) is rather cumbersome. To simplify the expressions, we confine the numerator and the denominator to the terms linear in the interaction constants $V^{\alpha_1\alpha_1}$ and $V^{\alpha_0\alpha_0}$ and neglect the constants $V^{\alpha_1\alpha_0}$ and $V^{\alpha_0\alpha_1}$ as rather small. As a result, we obtain

$$G^{L_0}_{\alpha_0,k,\alpha',p'+k'} = -\frac{a}{\Delta(\omega,k)}A^{L_0}_{\alpha_0,k,\alpha',p'+k'}, \quad (18a)$$

$$G^{L-L_0}_{\alpha_1,k,\alpha',p'+k'} =$$
$$= \frac{1}{\Delta(\omega,k)}(bA^{L_0}_{\alpha_1,k,\alpha',p'+k'} - cA^{L-L_0}_{\alpha_1,k,\alpha',p'+k'}), \quad (18b)$$

$$G^{L_0}_{\alpha_1,k,\alpha',p'+k'} =$$
$$= \frac{1}{\Delta(\omega,k)}(dA^{L-L_0}_{\alpha_1,k,\alpha',p'+k'} - eA^{L_0}_{\alpha_1,k,\alpha',p'+k'}), \quad (18c)$$

$$\Delta(\omega,k) = -\Big[1 - f^{L_0L_0}_{\alpha_0}(\omega,k)V^{\alpha_0\alpha_0} +$$
$$+ f^{L-L_0,L_0}_{\alpha_1}(\omega,k)V^{\alpha_1\alpha_1} + f^{L_0,L}_{\alpha_0}(\omega,k)V^{\alpha_1\alpha_1}\Big], \quad (19)$$

where the following notations were used:

$$a = 1 + f^{L-L_0,L}_{\alpha_0}(\omega,k)V^{\alpha_1\alpha_1} + f^{L_0,L}_{\alpha_0}(\omega,k)V^{\alpha_1\alpha_1},$$

$$b = f^{L-L_0,L}_{\alpha_0}(\omega,k)V^{\alpha_1\alpha_1},$$

$$c = 1 + f^{L_0,L}_{\alpha_0}(\omega,k)V^{\alpha_1\alpha_1} + f^{L_0,L_0}_{\alpha_0}(\omega,k)V^{\alpha_0\alpha_0},$$

$$d = f^{L_0,L_0}_{\alpha_1}(\omega,k)V^{\alpha_1\alpha_1},$$

$$e = [1 + f^{L-L_0,L_0}_{\alpha_1}(\omega,k)V^{\alpha_1\alpha_1}] + f^{L_0,L_0}_{\alpha_0}(\omega,k)V^{\alpha_0\alpha_0}.$$

Substituting Eqs. (18) and (19) into Eqs. (11), we obtain the expressions for Fourier components of the corresponding GF. The result of calculation shows that the Fourier components of the GF are proportional to the δ-function, $\delta_{k,k'}$. Therefore, the conservation law for the wave vector is fulfilled in this crystalline structure. As was marked in Introduction and is shown in Fig. 2, the wave vector changes in the narrower limits, $-\pi/(aL_j) \leqslant k_j \leqslant \pi/(aL_j)$. In addition, it is clear that, owing to the corresponding anharmonic terms, the dispersion curves describing the major vibrations have to split at the point of their intersection, $k_j = 0$.

3. Numerical Calculations and Analysis of Experimental Results

The expressions obtained for the FG, if being substituted into Eq. (5), make it possible to obtain the dependence of the Raman scattering spectra on the frequency and crystal parameters. In order to simplify expression (5) and to make the numerical simulation more convenient, the dependence of the susceptibility tensor on the wave vector will be neglected, assuming that $\tilde{\chi}^{s_j}_{k',\lambda',k,\lambda}(b_g + Q) = \tilde{\chi}^{s_j}_{k',\lambda',k,\lambda}$ at $k - k' = Q \to 0$. Then the Raman spectrum intensity is a sum of four terms:

$$I_{p',\lambda',p,\lambda}(\omega) \sim -[1 + n(\omega)]\mathrm{Im}\{I^{00}_{p',\lambda',p,\lambda} +$$
$$+ I^{01}_{p',\lambda',p,\lambda} + I^{10}_{p',\lambda',p,\lambda} + I^{11}_{p',\lambda',p,\lambda}\}, \quad (20)$$

where

$$I^{00}_{p',\lambda',p,\lambda} = \tilde{\chi}^{\alpha_0}_{k',\lambda',k,\lambda}\tilde{\chi}^{*\alpha_0}_{k',\lambda',k,\lambda}\{f^{L_0,L_0}_{\alpha_0}(\omega,Q) +$$
$$+ \frac{V^{\alpha_0,\alpha_0}a}{\Delta(\omega,Q)}f^{L_0,L_0}_{\alpha_0}(\omega,Q)f^{L_0,L_0}_{\alpha_0}(\omega,Q)\}, \quad (21a)$$

$$I^{01}_{p',\lambda',p,\lambda} = \tilde{\chi}^{\alpha_0}_{k',\lambda',k,\lambda}\tilde{\chi}^{*\alpha_1}_{k',\lambda',k,\lambda}\frac{V^{\alpha_1,\alpha_0}}{\Delta(\omega,Q)}f^{L_0,L_0}_{\alpha_0}(\omega,Q)\times$$
$$\times\left\{\frac{(a^L_Q - a^{L_0}_Q)d\tilde{\omega}_{\alpha_1,Q}}{\Delta(\omega,Q,\alpha_1)} + \frac{a^{L_0}_{p'+k'}\tilde{\omega}_{p'+k',\alpha_1}e}{\Delta(\omega,Q,\alpha_1)} - \right.$$
$$\left. - f^{L-L_0,L_0}_{\alpha_1}(\omega,Q)d\right\}, \qquad (21b)$$

$$I^{10}_{p',\lambda',p,\lambda} = \tilde{\chi}^{\alpha_1}_{k',\lambda',k,\lambda}\tilde{\chi}^{*\alpha_0}_{k',\lambda',k,\lambda}\frac{V^{\alpha_0,\alpha_1}}{\Delta(\omega,Q)}f^{L_0,L_0}_{\alpha_0}(\omega,Q)\times$$
$$\times\left\{\frac{(a^{L_0}_Q - a^{*L_0}_Q)\tilde{\omega}_{\alpha_1,Q}a}{\Delta(\omega,Q,\alpha_1)} - f^{L_0,L-L_0}_{\alpha_1}(\omega,Q)\right\}, \qquad (21c)$$

$$I^{11}_{p',\lambda',p,\lambda} = \tilde{\chi}^{\alpha_1}_{k',\lambda',k,\lambda}\tilde{\chi}^{*\alpha_1}_{k',\lambda',k,\lambda}\left(\frac{[1-a^{L_0}_0 - a^{*L_0}_0]\tilde{\omega}_{\alpha_1,Q}}{\Delta(\omega,Q,\alpha_1)} + \right.$$
$$+ f^{L_0,L_0}_{\alpha_1}(\omega,Q) - \frac{V^{\alpha_1,\alpha_1}}{\Delta(\omega,Q)}\left\{\frac{\tilde{\omega}_{\alpha_1,Q}}{\Delta(\omega,Q,\alpha_1)}\times\right.$$
$$\times\left[a^{*L_0}_Q\left(\frac{b(a^L_Q - a^{L_0}_Q)\tilde{\omega}_{\alpha_1,Q}}{\Delta(\omega,Q,\alpha_1)} - bf^{L-L_0,L_0}_{\alpha_1}(\omega,Q)\right)+\right.$$
$$+ a^{*L_0}_Q\left(\frac{ca^{L_0}_Q\tilde{\omega}_{\alpha_1,Q}}{\Delta(\omega,Q,\alpha_1)} - cf^{L_0,L_0}_{\alpha_1}(\omega,Q)\right)+$$
$$a^{*L}_Q\left(\frac{ea^{L_0}_Q\tilde{\omega}_{\alpha_1,Q}}{\Delta(\omega,Q,\alpha_1)} - ef^{L_0,L_0}_{\alpha_1}(\omega,Q) + \right.$$
$$\left.\left.+\left(\frac{d(a^L_Q - a^{L_0}_Q)\tilde{\omega}_{\alpha_1,Q}}{\Delta(\omega,Q,\alpha_1)} - df^{L-L_0,L_0}_{\alpha_1}(\omega,Q)\right)\right]-\right.$$
$$-\left[f^{L_0,L_0}_{\alpha_1}(\frac{b(a^L_Q - a^{L_0}_Q)\tilde{\omega}_{\alpha_1,Q}}{\Delta(\omega,Q,\alpha_1)} - bf^{L-L_0,L_0}_{\alpha_1}(\omega,Q)) + \right.$$
$$+ f^{L_0,L_0}_{\alpha_1}\left(\frac{ca^{L_0}_Q\tilde{\omega}_{\alpha_1,Q}}{\Delta(\omega,Q,\alpha_1)} - cf^{L_0,L_0}_{\alpha_1}(\omega,Q)\right)-$$
$$- f^{L_0,L}_{\alpha_1}\left(\frac{ea^{L_0}_Q\tilde{\omega}_{\alpha_1,Q}}{\Delta(\omega,Q,\alpha_1)} - ef^{L_0,L_0}_{\alpha_1}(\omega,Q)\right)+$$
$$\left.\left.\left.+ f^{L_0,L}_{\alpha_1}(\frac{d(a^L_Q - a^{L_0}_Q)\tilde{\omega}_{\alpha_1,Q}}{\Delta(\omega,Q,\alpha_1)} - df^{L-L_0,L_0}_{\alpha_1}(\omega,Q))\right]\right\}\right). \qquad (21d)$$

This formula is more exact than the formula presented in our work [30], because it includes the terms V^{α_1,α_1} and V^{α_0,α_0} not only in the constants in expressions (18) and (19), but also in the denominator $\Delta(\omega,Q)$. The following limiting cases can be distinguished for expression (20):

a) If the constants V^{α_0,α_0} and V^{α_1,α_1} of interaction between phonon branches are small, Eq. (20) is reduced to a simpler form, and the intensity, as in work [30], is described by two terms

$$I^{00}_{p',\lambda',p,\lambda} + I^{11}_{p',\lambda',p,\lambda} =$$
$$= \tilde{\chi}^{\alpha_0}_{k',\lambda',k,\lambda}\tilde{\chi}^{*\alpha_0}_{k',\lambda',k,\lambda}f^{L_0,L_0}_{\alpha_0}(\omega,Q) + \tilde{\chi}^{\alpha_1}_{k',\lambda',k,\lambda}\tilde{\chi}^{*\alpha_1}_{k',\lambda',k,\lambda}\times$$
$$\times\left[\frac{(1-a^{L_0}_0 - a^{*L_0}_0)\tilde{\omega}_{\alpha_1,Q}}{\Delta(\omega,Q,\alpha_1)} + f^{L_0,L_0}_{\alpha_1}(\omega,Q)\right], \qquad (22a)$$

b) If $V^{\alpha_0,\alpha_0} \gg V^{\alpha_1,\alpha_1}$, the scattering intensity is described by an equation similar to Eq. (22a), but the first term in Eq. (22a) changes and, in accordance with Eq. (20), is equal to

$$I^{00}_{p',\lambda',p,\lambda} = \tilde{\chi}^{\alpha_0}_{k',\lambda',k,\lambda}\tilde{\chi}^{*\alpha_0}_{k',\lambda',k,\lambda}f^{L_0,L_0}_{\alpha_0}(\omega,Q)/$$
$$/[1 - V^{\alpha_0,\alpha_0}f^{L_0,L_0}_{\alpha_0}(\omega,Q)] = \tilde{\chi}^{\alpha_0}_{k',\lambda',k,\lambda}\tilde{\chi}^{*\alpha_0}_{k',\lambda',k,\lambda}\times$$
$$\times\frac{\sum\limits_p a^{L_0}_{p+Q}a^{L_0}_{p+Q}\tilde{\omega}_{p+Q,\alpha_0}}{\omega^2 - V^{\alpha_0,\alpha_0}\sum\limits_p a^{L_0}_{p+Q}a^{*L_0}_{p+Q}\tilde{\omega}_{p+Q,\alpha_0}}, \qquad (22b)$$

c) If the QD size is close to the dimensions of new crystal cell ($L_0 \to L$), we obtain

$$I^{00}_{p',\lambda',p,\lambda}\tilde{\chi}^{\alpha_0}_{k',\lambda',k,\lambda}\tilde{\chi}^{*\alpha_0}_{k',\lambda',k,\lambda}\frac{\omega_{Q,\alpha_0}}{\omega^2 - \omega^2_{Q,\alpha_0}}, \qquad (22c)$$

d) If $L_0 \to 0$, all terms in Eqs. (21), (22a), and (22b), which are proportional to $a^{L_0}_{g+Q} \to 0$, vanish. Only the term corresponding to the matrix – this is the second term in Eq. (22a) – survives.

It is worth to note that the obtained relations for the Raman scattering intensity can describe the processes with participation of both acoustic and optical phonons. The scattering regularities depend on the dispersion character of phonon branches. In the following part, we analyze the results of numerical calculations only for light scattering by phonons provided that the convolution of the acoustic phonon branches takes place, and compare the corresponding results with experiment data.

As one can see from Eqs. (21), (22a), and (22b), the intensity of Raman scattering spectra depends on functions of the types $f^{L_0,L_0}_{\alpha_1}(\omega,Q)$ and $f^{L_0,L_0}_{\alpha_0}(\omega,Q)$, and has resonance (12) near a certain value of the frequency that enters into $\Delta(\omega,g+Q,\alpha) = \omega^2 - \eta\omega_{g+Q,\alpha}\tilde{\omega}_{g+Q,\alpha}$. The dimensions of Ge quantum dots in the SL satisfy the condition $L_x, L_y \gg L_z$. Therefore, as was shown in Appendix 1 of our work [30], only the coordinate z in the functions $f^{L_0,L_0}_{\alpha_j}(\omega,Q)$ is important. For acoustic phonons, the bulk crystal branches can be well described by the expression $\omega_{g+Q,\alpha} = \left|\omega_{0,\alpha}\sin[\frac{a(b_{z,g}+Q_z)}{2}]\right|$, where a

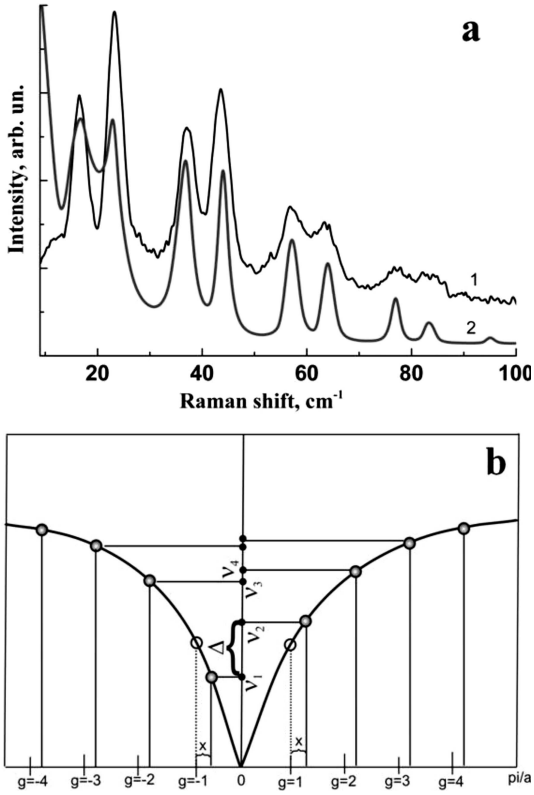

Fig. 3. Experimental Raman spectrum (*1*) for a multilayer structure with Ge quantum dots and the corresponding theoretical spectrum (*2*) calculated on the basis of the proposed model with the fitting parameters $V^{\alpha_1\alpha_1} = V^{\alpha_0\alpha_0} = 4$ cm^{-2} (*a*). Schematic explanation of the emergence of a doublet in Raman spectra (*b*)

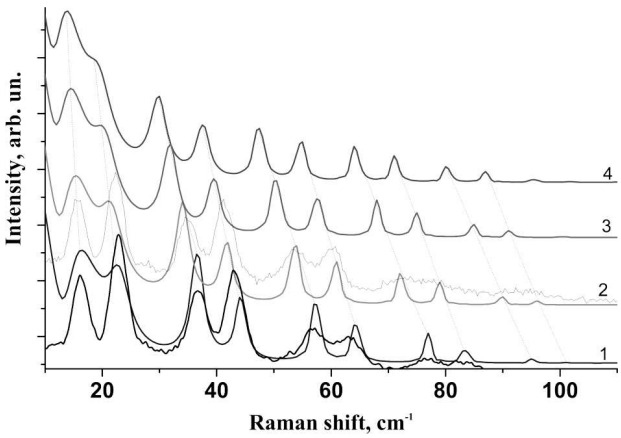

Fig. 4. Theoretical Raman spectra of multilayer structures with QDs with a fixed height of 1.5 nm and the thickness of a Si layer varying from 10 (curve *1*) to 16 nm (curve *4*). For the sake of comparison, experimental Raman spectra are shown for the first two theoretical spectra

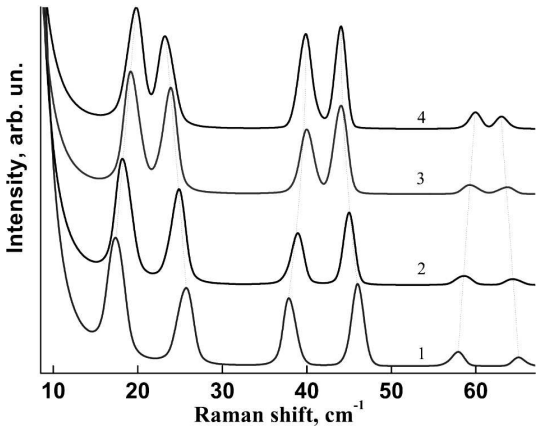

Fig. 5. Theoretical Raman spectra of multilayer structures (the thickness of Si layers is fixed) with QDs (the height of QDs is fixed) for various exciting radiation wavelengths: 350 (*1*), 450 (*2*), 650 (*3*), and 750 nm (*4*)

is the lattice constant, Q the wave vector of light, and g a new reciprocal lattice vector ($b_{z,g} = \frac{2\pi}{aL_z} g_{z,i}$, $-\frac{L_z}{2} \leqslant g_{z,i} \leqslant \frac{L_z}{2}$, $g_{z,i} = 0, \pm 1, \pm 2$). If the light wave vector is neglected, i.e. $Q \to 0$, the peak of resonance (22a) should take place at $g_{z,i}$. As is seen from Fig. 3, *b*, the positions and intensities of both peaks should be identical for $\pm g_{z,i}$ and $Q \to 0$. However, the positions and the intensities of two peaks described above are different if $Q \neq 0$. Really, $\pm b_{z,g} + Q_z = \frac{2\pi}{aL_z}(\pm g_{z,i} + \frac{aL_z n}{\lambda})$. Therefore, if L_z or the refractive index n is large, the contribution of the second term in the parentheses is considerable, and the band doublets rather than single bands should be observed in the spectrum in this case, which is well illustrated in Fig. 3, *b*. The doublet splitting depends on the parameters λ, L_z, and n. The numerical analysis of some cases calculated at a variation of main parameters and the comparison of the obtained results with experimental data are exhibited in Figs. 3 to 5.

In Fig. 3, *a*, the experimental (curve *1*) and calculated (curve *2*) Raman spectra for a 10-layer SL with Ge quantum dots are shown. One can see that the intensities of doublets and the frequency positions of bands are well described by the theoretical spectrum. Other theoretical curves in Fig. 4 illustrate the influence of the Si layer thickness, provided that all other SL parameters are identical. When the layer thickness increases from 10 to 16 nm, the spectrum

center-of-mass shifts toward lower frequencies and the distance between the bands in the doublet slightly increases. Such spectral variations are explained in the framework of the proposed model by the growth of the parameter L_z. Therefore, they are associated with the increase in the number of intersection points in the dispersion curve (Fig. 2). Hence, provided that the wavelength of exciting laser radiation that corresponds to phonons with analogous wave vectors is fixed, the frequencies of corresponding spectral bands change according to the dispersion curve variations.

Figure 5 illustrates the effect produced by a variation of the exciting radiation wavelength λ_{exc}. One can see that, when the excitation energy changes from 1.65 eV ($\lambda_{\text{exc}} = 750$ nm) to 3.55 eV ($\lambda_{\text{exc}} = 350$ nm), the distance between the doublet bands decreases, but the position of the doublet center remains invariant. It should be noted that the best fitting of theoretical spectra to experimental ones is obtained at rather small values of interaction constants ($V^{\alpha_0,\alpha_0}/\omega_{\alpha_0}$ and $V^{\alpha_1,\alpha_1}/\omega_{\alpha_1} \leqslant 0.05$).

It should also be emphasized that, as was shown in works [33, 34], the real QDs have a mixed Si–Ge composition, which is caused by a giant interdiffusion of Si from the silicon substrate owing to nonuniform stresses in vicinities of QDs. One can evaluate the component composition in QDs from the Raman spectra of scattering by optical phonons. Really, the frequencies of the Ge–Ge, Si–Ge, and Si–Si vibration modes in the Si–Ge solid solution substantially depend on the content of each component. The account of the effect of component mixing allows the Raman spectra of light scattering by the convolutions of acoustic phonon dispersion branches to be described more precisely.

4. Conclusions

A theoretical simulation of Raman spectra experimentally obtained in multilayered structures with quantum dots is carried out. It is shown that the theoretical description of the Raman spectra (or absorption ones) for such structures should consider the growth of the number of phonon modes. A model for the description of experimental Raman spectra of the structures concerned is proposed, which involves the real crystal structure in both the QDs and the surrounding matrix, as well as the interaction between the QD vibrations and matrix phonons. By using the secondary quantization procedure and the Green's function method, the frequency dependence of the Raman spectrum intensity is calculated. The obtained results show that the crystal structures of superlattices with quantum dots can be described as mixed crystals with a certain distribution of impurities assembled in large "Ge molecules" (QDs). It is shown that a qualitative correlation between the positions and the intensities of bands in theoretical and experimental Raman spectra is observed at certain values of SL parameters. The emergence of characteristic band doublets is explained.

The authors are grateful to A.V. Novikov (the Institute for Physics of Microstructures of the Russian Academy of Sciences) for experimental specimens.

1. K.L. Wang, D. Cha, J. Liu, and C. Chen, Proc. IEEE **95**, 1866 (2007).
2. D.H. Feng, Z.Z. Xu, T.Q. Jia, X.X. Li, and S.Q. Gong, Phys. Rev. B **68**, 035334 (2003).
3. E. Finkman, N. Shuall, A. Vardi, V. Le Thanh, and S.E. Schacham, J. Appl. Phys. **103**, 093114 (2008).
4. A.S. Barker, jr., J.L. Merz, and A.C. Gossard, Phys. Rev. B **17**, 3181 (1978).
5. Sung-kit Yip and Yia-Chung Chang, Phys. Rev. B **30**, 7037 (1984).
6. C. Colvard, R. Merlin, M.V. Klein, and A.C. Gossard, Phys. Rev. Lett. **45**, 298 (1980).
7. B. Djafari-Rouhani, L. Dobrzynski, O.H Duparc, R.E. Camely, and A.A. Maradudin, Phys. Rev. B **28,** 1711 (1983).
8. B. Jusserand, D. Paquet, F. Mollot, F. Alexandre, and G. Le Roux, Phys. Rev. B **35**, 2808 (1987).
9. J. Zi, K. Zhang, and X. Xie, Progr. Surf. Sci. **54**, 69 (1997).
10. S.M. Rytov, Akust. Zh. **2**, 71 (1956).
11. P.A. Knipp and T.L. Reinecke, Phys. Rev. B **46**, 10 310 (1992).
12. A.K. Sood, J. Menendez, M. Cardona, and K. Ploog, Phys. Rev. Lett. **54**, 2111 (1985).
13. V.I. Belitsky, T. Ruf, J. Spitzer, and M. Cardona, Phys. Rev. B **49**, 8263 (1994).
14. A.J. Shields, M. Cardona, and K. Eberl, Phys. Rev. Lett. **72**, 412 (1994).
15. M. Grundmann, O. Steir, and D. Bimberg, Phys. Rev. B **52**, 11969 (1995).
16. K. Yip and Y.-C. Chang, Phys. Rev. B **30**, 7037 (1984).
17. M.C. Klein, F. Hache, D. Ricard, and C. Flytzanis, Phys. Rev. B **42**, 11123 (1990).
18. E. Duval, Phys. Rev. B **46**, 5795 (1992).
19. C. Trallero-Giner, A. Debernardi, M. Cardona, E. Menendez-Proupin, and A.I. Ekimov, Phys. Rev. B **57**, 4664 (1998).

20. M. Cazayous, J.R. Huntzinger, J. Groenen, A. Mlayah, S. Christiansen, H.P. Strunk, O.G. Schmidt, and K. Eberl, Phys. Rev. B **62**, 7243 (2000).
21. M. Cazayous, J. Groenen, J.R. Huntzinger, A. Mlayah, and O.G. Schmidt, Phys. Rev. B **64**, 033306 (2001).
22. H. Fu, V. Ozolins, and A. Zunger, Phys. Rev. B **59**, 2881 (1999).
23. S.-F. Ren, Z.-Q. Gu, and D. Lu, Solid State Commun. **113**, 273 (2000).
24. M.I. Vasilevskiy, Phys. Rev. B **66**, 195326 (2002).
25. M. Cazayous, J. Groenen, A. Zwick, A. Mlayah, R. Carles, J.L. Bischoff, and D. Dentel, Phys. Rev. B **66**, 195320 (2002).
26. A.G. Milekhin, A.I. Nikiforov, O.G. Pchelyakov, S. Schulze, and D.R.T. Zahn, Nanotechnology **13**, 55 (2002).
27. P.D. Lacharmoise, A. Bernardi, A.R. Goni, M.I. Alonso, M. Garriga, N.D. Lanzillotti-Kimura, and A. Fainstein, Phys. Rev. B **76**, 155311 (2007).
28. G. Zanelatto, Yu.A. Pusep, N.T. Moshegov, A.I. Toropov, P. Basmaji, and J.C. Galzerani, J. Appl. Phys. **86**, 4387 (1999).
29. J.R. Huttinger, A. Mlayah, V. Paillard, A. Wellner, N. Combe, and C. Bonafos, Phys. Rev. B **74**, 115308 (2006).
30. V.O. Yukhymchuk, V.M. Dzhagan, A.M. Yaremko, and M.Ya. Valakh, Eur. Phys. J. B **74**, 10 (2010).
31. H.J. Benson and D.L. Mills, Phys. Rev. B **1**, 4835 (1970).
32. A.M. Yaremko, V.V. Koroteev, V.O. Yukhymchuk, V.M. Dzhagan, H. Ratajczak, A.J. Barnes, and B. Silvi, Chem. Phys. **388**, 57 (2011).
33. Z.F. Krasilnik, P.M. Lytvyn, D.N. Lobanov, N. Mestres, A.V. Novikov, J. Pascual, M.Ya. Valakh, and V.A. Yukhymchuk, Nanotechnology **13**, 81 (2002).
34. M.Ya. Valakh, V.O. Yukhymchuk, V.M. Dzhagan, O.S. Lytvyn, A.G. Milekhin, A.I. Nikiforov, O.P. Pchelyakov, F. Alsina, and J. Pascual, Nanotechnology **16**, 1464 (2005).

Received 04.03.15.
Translated from Ukrainian by O.I. Voitenko

Ю.А. Романюк, А.М. Яремко,
В.М. Джаган, В.О. Юхимчук

КОМБІНАЦІЙНЕ РОЗСІЮВАННЯ СВІТЛА
В НАДҐРАТКАХ З Ge КВАНТОВИМИ ТОЧКАМИ

Р е з ю м е

Проведено дослідження надґраток (НГ) з шарами Ge квантових точок (КТ) методом комбінаційного розсіювання світла (КРС) та запропоновано теоретичну модель, що описує експериментальні спектри. Модель враховує реальну кристалічну структуру КТ та навколишньої матриці, а також фонон-фононну взаємодію КТ з матрицею. Інтенсивності спектрів КРС розраховувалися з використанням процедури вторинного квантування та методу функцій Гріна. Отримані результати показали, що кристалічна структура надґратки, що складається з кремнієвих шарів та шарів з Ge квантовими точками, може бути описана як змішаний кристал з певним розподілом "домішок" (Ge-"молекул"). Продемонстровано якісну кореляцію в положенні та інтенсивності смуг у теоретично розрахованих та експериментально отриманих спектрах КРС від надґраток з шарами Ge (SiGe) квантових точок та пояснено дублетний характер смуг.